Toward printing molecular nanostructures from microstructured samples in ultrahigh vacuum

Christophe Nacci, Alex Saywell, Cedric Troadec, Jie Deng, Marc Georg Willinger, Christian Joachim, and Leonhard Grill

Toward printing molecular nanostructures from microstructured samples in ultrahigh vacuum

Christophe Nacci
Department of Physical Chemistry, Fritz-Haber-Institute of the Max-Planck-Society, 14195 Berlin, Germany and Department of Physical Chemistry, University of Graz, 8010 Graz, Austria

Alex Saywell
Department of Physical Chemistry, Fritz-Haber-Institute of the Max-Planck-Society, 14195 Berlin, Germany and School of Physics and Astronomy, The University of Nottingham, Nottingham NG7 2RD, United Kingdom

Cedric Troadec and Jie Deng
Institute of Materials Research and Engineering (IMRE), Agency for Science, Technology and Research (A*STAR), 2 Fusionopolis Way, #08-03 Innovis, Singapore 138634

Marc Georg Willinger
Department of Inorganic Chemistry, Fritz-Haber-Institute of the Max-Planck-Society, 14195 Berlin, Germany

Christian Joachim
Nanosciences Group and MANA Satellite, CEMES-CNRS, 31055 Toulouse, France and International Center for Materials Nanoarchitectonics (MANA), National Institute for Materials Science (NIMS), 1-1 Namiki, Tsukuba, Ibaraki 305-0044, Japan

Leonhard Grill[a)]
Department of Physical Chemistry, Fritz-Haber-Institute of the Max-Planck-Society, 14195 Berlin, Germany and Department of Physical Chemistry, University of Graz, 8010 Graz, Austria

Transferring molecular nanostructures from one surface to another in ultrahigh vacuum (UHV) by mechanical contact might be a possible route to avoid the severe limitations of *in situ* molecular synthesis on technologically relevant template surfaces. Here, transfer printing in UHV of molecular structures between metal surfaces is investigated by a combination of scanning tunneling microscopy and scanning electron microscopy/energy dispersive x-ray spectroscopy. The authors present the complete procedure of the printing and characterization process. Microstructured Au-coated MoS_2 samples exhibiting a periodic pillar structure are used as *stamp* surfaces with Au(111) single crystals as *target* surface. Polymers of 1,3,5-tris(4-bromophenyl)benzene molecules and graphene nanoribbons with an armchair edge structure are grown on the pillars of the stamp surface. After bringing the two surfaces in mechanical contact, the transferred material is found on the target while decapping occurs on the stamp surface. Polymer structures are probably buried under the transferred stamp material, and in rare cases, evidence for molecular structures is found in their vicinity. © 2015 American Vacuum Society. [http://dx.doi.org/10.1116/1.4936886]

I. INTRODUCTION

The deposition of large molecular nanostructures, and, in particular, molecular wires onto—potentially prestructured—surfaces, under ultraclean conditions is an important challenge for nanotechnology and in molecular electronics.[1] This is due to the large molecular mass of the expected molecular nanocircuits and consequently to the low vapor pressures that prohibit the use of conventional thermal sublimation under vacuum conditions because they would dissociate before a substantial sublimation rate is reached.[2,3] On the other hand, large molecular nanostructures are only soluble if equipped with long side groups that can perturb their shape and functionality.[4,5] For this reason, the covalent linking of molecular building blocks to form large molecular nanostructures in a bottom-up approach directly on a surface—the so-called on-surface polymerization—has become

a popular field in the last years.[6,7] This technique can be used to build *a priori* insoluble nanostructures that might have a strong impact in the field of nanomaterials and in molecular electronics.[8,9] However, although many examples of on-surface polymerization have been reported in the last years on metallic surfaces,[10–17] there are very few successful examples on more technologically relevant nonmetallic substrates, for instance, semiconductor or oxide surfaces,[18,19] which are advantageous to electronically decouple the molecules from the surface. A successful polymerization process requires a full control of the balance between the dehalogenation step and the diffusion of molecular species on the surface, because these two properties determine the efficiency of the chemical reaction and consequently the outcome of the entire process. This is more challenging for semiconductor surfaces where the high surface reactivity typically suppresses molecular diffusion. The surface can also offer additional (undesired) reaction channels for the molecules with the surface itself or even induce molecular

---

[a)]Electronic mail: Leonhard.grill@uni-graz.at

defragmentation.[20] On the other hand, the passivation of semiconductor surfaces might cause problems for the polymerization process, due to the weak molecular adsorption that could lead to desorption while attempting thermal activation of the on-surface polymerization. Heating treatments might also be detrimental to the template itself by decomposition effects.

Due to these problems of on-surface polymerization on technologically relevant surfaces (and the deposition and solubility problems with molecular wires), printing of molecular wires from one surface to another under ultrahigh vacuum conditions represents a promising alternative route that could help to bypass the above-mentioned issues and allow efficient transfer. In this approach, molecular wires are assembled on one sample and then transferred by mechanical contact to a technologically more relevant one, where the polymerization might not be efficient. So far, the transfer printing of nanoscale objects from one surface to another surface has been done only with metallic nanowires and metallic nanoislands.[21] The printing was done by gently pressing a stamp toward different surfaces, allowing the transfer of 8% of the nanoislands.

Another "transfer-material" strategy is based on preparing the material to be transferred on a sacrificial substrate, i.e., removing it by etching after the procedure, for instance, a thin (typically 100 nm) Ni film.[22] Recently, the adhesive properties of thin organic molecular layers, e.g., C_{60} multilayers, have been exploited to strip metal Au layers (support template) by mechanical peeling[23] from a Mica substrate. Bidimensional molecular organic layers grown on Au/Mica have been covered with 10–100 nm C_{60} layers and then polydimethylsiloxylane (PDMS).[23] The C_{60} layer acts as a protective and adhesive layer that allows to mechanically peel the Au layer from the Mica substrate. This results in a molecular organic layer sandwiched between the Au layer on one side and C_{60} (plus PDMS) on the other side. The Au layer can be removed by a chemical process leaving the molecular nanostructures and fullerenes exposed. This surface is then ready to be brought into mechanical contact to a target template, e.g., SiO_2, for transferring either molecular nanostructures or part of the fullerene layer in ambient environment. In these cases, graphene[22] and porphyrin molecules[23] have been investigated by Raman and fluorescence spectroscopies before and after printing. The characteristic bands and emission peaks are left unperturbed by the printing process, suggesting that the structures are preserved after transferring them to another surface. The same approach has been used by Cai *et al.*[8] that reported the growth and transfer of graphene nanoribbons from Au(111) to a SiO_2/Si substrate surface by repeated gentle pressing of target and stamp surfaces against each other. The graphene nanoribbon (GNR) transfer has been studied by Raman spectroscopy.[8] However, no microscopic methods have been used in these cases to identify individual molecular structures and the molecular intactness after transfer by printing nor the atomic scale cleanness of the remaining surface. Note that, on the other hand, the transfer of much larger graphene flakes has been intensely studied in the last years.[24,25]

On the other hand, Deng *et al.* achieved the transfer of triangular Au nanoislands from a microstructured MoS_2 stamp surface to different flat target surfaces, i.e., H-passivated Si(100), Mica, SiO_2, and graphite via an UHV-printing scheme.[26] The efficiency of the transfer as a function of the pillar area has been evaluated by analyzing stamp and target surfaces by SEM before and after the transfer. The preservation of the shape and the structure of Au nanoislands has been verified by analyzing and comparing transmission electron microscopy cross-sectional images of Au-nanoislands on MoS_2 and on Si(100)H, i.e., before and after the printing process, respectively.[27] However, a successful transfer of molecular structures under UHV conditions with a microscopy study of the target surface afterwards is still missing.

All studies mentioned above are applications of different printing schemes based on the use of flat or microstructured *stamp* surfaces and achieved in different environments such as ambient and UHV. Importantly, these methods reveal a poor spatial control of the material transfer and not always a clear assessment of the transfer efficiency. Here, we report on printing attempts of covalently linked nanostructures grown on a periodic pillar matrix by on-surface synthesis in UHV environment. As an important novelty, we use pillars on the source sample with a significantly reduced area ($1 \ \mu m^2$) as compared to previous attempts ($25 \ \mu m^2$). This should allow spatially confined (and well-defined) areas for the molecular transfer.

So far, most studies characterized the transferred material (before and after printing) only by spectroscopy techniques (mainly, Raman and fluorescence spectroscopies) that average over large sample surface areas. Here, we are using microscopy techniques, mainly STM, to characterize the molecular nanostructures before and after printing. STM is a powerful technique that allows a complete characterization of the structure and electronic properties of the nanostructures at the level of single atoms and molecules.[28,29] Since the search for printed nanostructures by STM can be very time-consuming, due to printing contact only in limited areas of the sample, and in order to perform the printing in the most efficient way, the STM characterization has been complemented by investigating the *stamp* and *target* surfaces by SEM and energy dispersive x-ray spectroscopy (EDX), thus at much larger length scales.

II. EXPERIMENTAL SETUP

The MoS_2 substrates were obtained from (commercial) large (2 cm in lateral size with a thickness of about 3 mm) natural crystals, which were exfoliated with a scotch tape before the microlithography procedure. The cleaved crystal provides a very flat surface since the typical terrace size of MoS_2 is about 100 μm (see supplementary material[30]). MoS_2 is a lamellar compound with weak van der Waals interactions between the S-Mo-S layers that can be easily cleaved in the [001] direction. Hence, microstamps with very small lateral dimensions are unlikely stable. MoS_2 sample surfaces were microstructured over an area of several squared millimeter by lithographic technique[26,27] to provide a periodic

arrangement of squared pillars, each with a lateral size of $1\,\mu m^2$. We fabricated microstructured samples with different pillar heights, i.e., 150 or 270 nm. The pillar top-surfaces are presumably the only areas involved in the *stamp–target* surfaces contact and consequently the locations where the molecular transfer will take place. The Au coating was performed under the same conditions used for the Au nanoislands,[26,27] except the thickness of the film deposited was increased to 47 nm to allow a full coverage of gold. This process should lead to the formation of a crystalline Au(111) film on and off the pillars.

Owing to its lamellar structure, MoS_2 can efficiently absorb the pressure contact while printing without breaking and therefore appears very suitable for such purpose.[27] It turned out that a periodic arrangement of microstamps fabricated on such a template (MoS_2) enhances the material transfer rate per area compared to a flat stamp surface.[27] This strategy offers the possibility to confine the transfer to well-defined surface locations of small size and moreover to identify the transferred material owing to the periodicity of the pillar network, but it has never been tested with molecular nanostructures so far.

STM measurements were conducted at room-temperature in UHV environment by using a Pt/Ir tip. STM measurements of both the *stamp* and *target* surfaces were combined with *ex situ* SEM imaging characterization and EDX elemental characterization. SEM analysis was performed using a Hitachi 4800 SEM. The instrument is equipped with a cold field emitter and a silicon drift detector from Bruker for EDX analysis.

The UHV printer is based on an ANPz100 (Attocube) positioner piezoelement. The stamp surface is mounted on top of the piezoelement and the target surface on a fixed receptor. The printer tool is built to bring the stamp and target surfaces into contact while providing a parallel surface-to-surface orientation configuration. To ensure optimal conditions for a parallel arrangement, the sample holders of the stamp and the target crystals are both mounted on sensitive springs when placed inside their respective receptors (the one mobile mounted on top of the nanopositioner and the other one fixed on the printer frame). Thus, after establishing a contact between the stamp and target surfaces and further pushing, the springs act to adjust the crystal positions to compensate, at least to some extent, an eventual angular misalignment between the target and stamp surface.

A saw-tooth signal (voltage amplitude: 30–50 V; signal frequency: 30–50 Hz) allows actuation of the piezo and the holder in a stick-slip motion and brings the two surfaces into contact while optically monitoring the gap between stamp and target surfaces. At the same time, the electric resistance between the two surfaces is measured to identify when a contact is established via the closing of the electric circuit. In detail, the procedure is the following: The nanopositioner moves constantly until the gap between the stamp and target surfaces is small but a contact not established yet. Then, the motion is activated by applying single voltage pulses until the contact is achieved and a small finite resistance ($<2\,\Omega$) between the two surfaces is measured. After establishing the

contact, the stamp was further pressed against the target surface by moving the nanopositioner via several pulses (from 50 to 500 pulses with the above-mentioned amplitude and frequency values). The stamp is then kept there for a few minutes until it is gently retracted by single steps and the electric contact is lost. This printing procedure is repeated several times within one experimental run. Note that a simultaneous contact of all stamp pillars with the target surface is unlikely, because target surface is not perfectly flat and the pillars do not all have exactly the same height. Accordingly, only a fraction of pillars of the stamp surface is expected to be in contact with the target surface during printing.

III. RESULTS AND DISCUSSION

A. Microstructured Au/MoS₂ surfaces (*stamp* surface)

The stamp surface is a MoS_2 substrate having a microstructured region extending over an area of about $4 \times 3\,mm^2$, as verified by optical microlithography.[27] A thin layer of Au (47 nm) was thermally deposited on this microstructured surface to enable in the subsequent step the growth of polymers via on-surface polymerization as has been done previously on Au surfaces.[31–34] The microstructured region consists of a periodic array of pillars with a lateral extension of $1\,\mu m^2$ and a height of about 250 nm (or 150 nm) as visible from the SEM micrographs in Fig. 1 (the distance between the two adjacent pillars, the so-called pitch, is $2\,\mu m$). Gold crystallites are grown on top of the pillars and in their surrounding

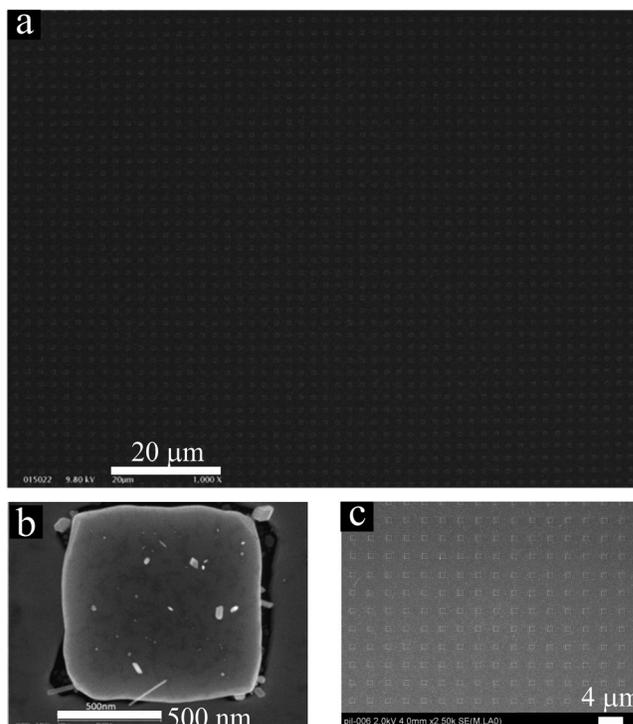Fig. 1. (a) Large view of a lattice of 51×38 submicron stamps microfabricated and Au metallized from a well cleaved and ultraflat MoS_2 surface wafer ($120 \times 90\,\mu m^2$ SEM image). (b) SEM image of an individual Au-coated MoS_2 pillar. Au crystallites are visible on the pillar top-surface and in the surrounding as well. As-delivered microstructured samples. (c) SEM image of the as-delivered microstructured sample shown in panel (a).
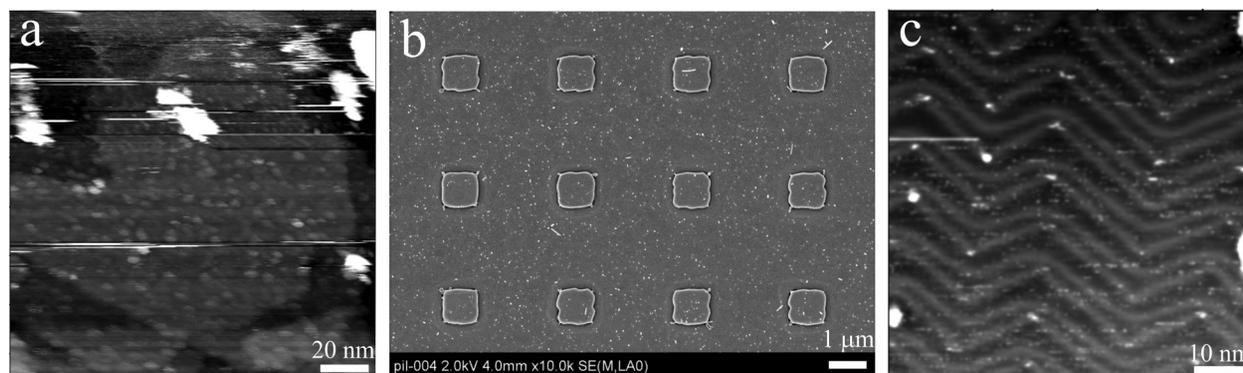
Fig. 2. (a) STM image of an as-delivered Au/MoS$_2$ microstructured surface (in-between pillars). (b) SEM image of the same sample in panel (a) after being conditioned by soft sputtering and annealing conditions. (c) STM image taken on top of a pillar of the sample shown in panel (b) showing the typical herringbone reconstruction of Au(111).

(between the pillars), as shown in the SEM image of a single pillar in Fig. 1(b). The samples have been prepared in-vacuum at IMRE (Singapore) and afterwards shipped to FHI-Berlin, thus being in air for at least one week. The Au/MoS$_2$ periodic microstructure remains unperturbed during shipping as clearly visible from the SEM micrograph in Fig. 1(c). Chemical species might adsorb on restricted areas such as the pillar top-surfaces, which could affect the molecular diffusion and result in large deviations of the expected area or length of the polymerized structures compared to the growth on typical large and extended terraces, i.e., in-between the pillars. An analysis of 1,3,5-tris(4-bromophe-nyl)benzene (TBPB) clusters area and GNR's length grown on top of the pillars and in-between the pillars does not show any particular difference between the two cases (see supplementary material[30]).

STM measurements in UHV (without any sample treat-ment) revealed a rough and nonreconstructed Au surface both on the top-surface of the pillar and in-between the pillars [see Fig. 2(a)]. Such a surface is not suitable for on-surface polymerization as cleanliness and atomic scale flat-ness are crucial requirements for efficient diffusion of the molecular monomers along the surface.

The microstructured sample surface was then processed by repeated soft-conditions sputtering/annealing cycles (sputter-ing conditions: 10 min, beam energy: 0.7 keV, and drain current $= 5.4\,\mu A$; annealing conditions: 10 min at 400 °C).

This UHV-cleaning left the pillars shape and its periodic arrangement unperturbed, as shown in Fig. 2(b). As a further consequence, the Au terminated microstructured stamp sur-face showed the typical herringbone reconstruction of a Au(111) surface [see Fig. 2(c)]. Hence, despite the transport of several days/weeks in air, a clean and microstructured gold surface, being atomically flat both between and on top of the pillars, could be achieved by a simple UHV preparation.

Individual pillars have been identified first, and then, their top-surface was imaged by STM, as shown in Fig. 3(a). The surface turns to be quite structured as visible from the appa-rent line profile taken across the pillar surface [see Fig. 3(b)] and the differentiate z height topography [Fig. 3(c)]. This roughness is ascribed to the formation of Au crystallites grown during the Au layer deposition.

B. On-surface synthesis on microstructured Au/MoS$_2$ surfaces

Two-dimensional covalently bound networks made of 1,3,5-tris(4-bromophenyl)benzene molecules (Br$_3$TBPB) were grown on the microstructured Au/MoS$_2$ stamp surface. Individual pillars have been first identified by STM and the top-surface imaged, as shown in Fig. 4(a). Br$_3$TBPB mole-cules were first deposited on the microstructured sample kept at room-temperature and then dehalogenated at a tem-perature of 490 K (sample heating for 5 min).[15,33] Large Au terraces (typically 100 nm wide) with a low coverage of
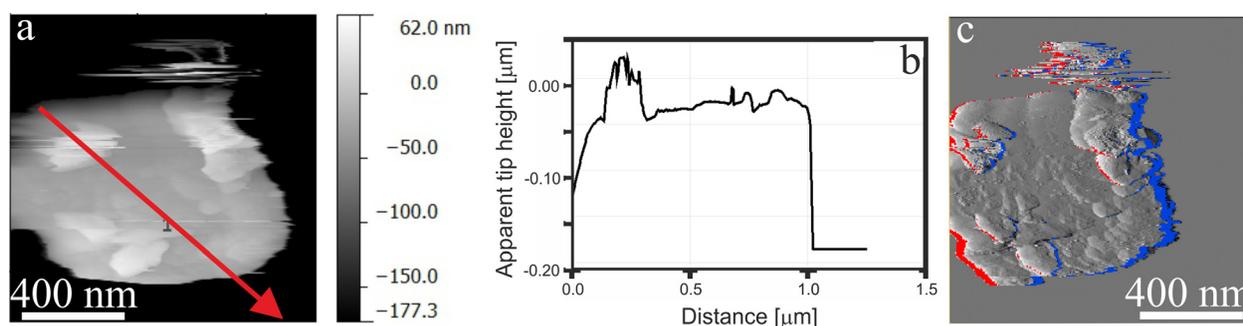

Fig. 3. (Color online) (a) STM image of a single Au/MoS$_2$ pillar, (b) apparent height line-profile across the pillar shown in (a) showing a height of almost 200 nm (the limited z scan range of the microscope makes a simultaneous imaging of the top-pillar surface and regions in between pillars nearly impossible). (c) Differential Z height STM topography of image in panel (a).
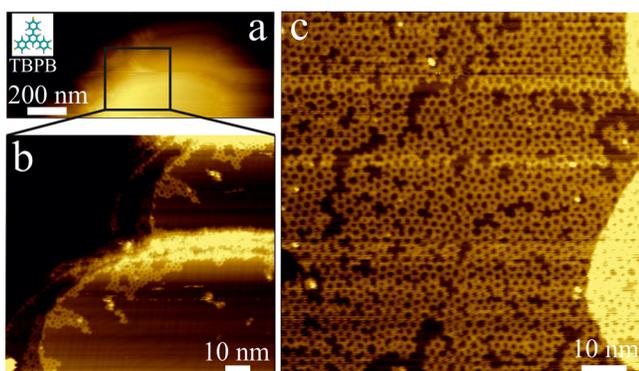
FIG. 4. (Color online) TBPB-based 2D-networks on Au/MoS$_2$ pillared surface by on-surface synthesis. (a) STM topography (2.5 V, 40 pA) of part of a Au/MoS$_2$ pillar ($1 \times 1 \times 0.27$ μm). The TBPB chemical structure is shown in the inset. (b) Zoom-in (2.5 V, 40 pA) of the area indicated by the black square in panel (a) showing low-coverage TBPB networks on the Au/MoS$_2$ pillar. (c) Large and extended TBPB networks on the microstructured surface after increasing the molecular coverage at the surface. STM image taken at set points (-2 V, 50 pA) and on the pillars.

covalently linked TBPB-based islands are found, as shown in Fig. 4(b). Depositing a higher molecular coverage results in extended polygonal covalently linked networks on top of the pillars, as shown in Fig. 4(c). Having a high molecular coverage on top of the microstamps should potentially be helpful in view of achieving an efficient material transfer by printing.

C. UHV-printing: Characterization of stamp and target surfaces by SEM and STM

The *stamp* surface was repeatedly brought into contact (in UHV) with a clean and well-prepared single crystal Au(111) surface (*target*), and subsequently, both surfaces were characterized by STM and SEM/EDX techniques. SEM characterization of the stamp and target surfaces might give important information at large scale, i.e., beyond our STM maximum lateral scan range (2 μm), about the printing process that otherwise are extremely difficult to get by STM only. Figure 5(a) shows an STM image of small TBPB network patches grown on a single Au(111) crystal surface. The same surface has been imaged *ex situ* by SEM. It is known that monolayers of carbon structures such as graphene[35] on a metal substrate or self-assembled monolayers of alkanethiolates on gold[36] can be detected through a change in secondary electron (SE) signal intensity. As shown in Fig. 5(b), SEM indeed reveals nonuniform structures of darker contrast across the surface. Their aspect is similar to the one observed in the STM overview image [Fig. 5(a)]. However, due to the limited spatial resolution of the SEM technique, it does not provide a conclusive evidence for the presence of molecular entities based on TBPB's (see supplementary material[30]) grown on the microstructured stamp surfaces.

SEM imaging of the Au(111) target surface reveals dark/bright stripes ascribed to the surface topography features such as terraces and surface steps [Fig. 6(a)] without any evidences for transferred pillars in the imaged areas. Some
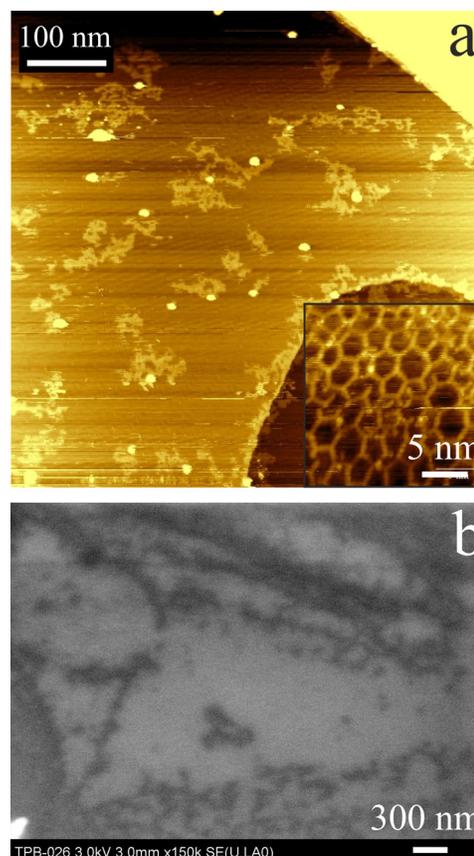

FIG. 5. (Color online) SEM characterization of TBPB networks on a flat Au(111) single crystal surface. (a) STM topography (-2 V, 30 pA) of small TBPB-islands grown on Au(111) surface by on-surface polymerization. The inset shows the typical internal structure of a TBPB-based island (-0.3 V, 10 pA). (b) SEM images of the surface shown in panel (a): the small darky-features might be associated either to TBPB networks or surface topographic features.

other areas show a pronounced deviation in the secondary electron image contrast [see Fig. 6(b)], indicating new features that can likely be assigned to transferred material. The pronounced SE contrast between the transferred material as compared to the Au surface was further investigated in terms of elemental composition by EDX spectroscopy. As shown in Figs. 6(b) and 6(d), they contain spectroscopic contributions from Mo and S elements according to the EDX spectra in Figs. 6(c), 6(e), and 6(f) leaving no doubt about the transfer of material from the stamp to the target surfaces.

As a further check, the stamp surface was imaged by SEM as well to reveal the effect of the printing process to the microstamps' area. Some regions of the pillared area show a clear and sharp change of the SE contrast, as discernible from Figs. 7(a)–7(b). At higher magnification, it turns out that these dark-contrast areas are nothing but areas of decapped pillars [see Fig. 7(b)] that are now MoS$_2$-terminated. The periodic distribution of pillars is locally disrupted, and thin capping layers are identified nearby. Clear contributions from Mo and S elements from decapped pillars and part of the capping layers nearby are detected from EDX spectra in Figs. 7(c) and 7(d).

This is another signature of the mechanical contact between the stamp and the target surfaces. Printing seems to
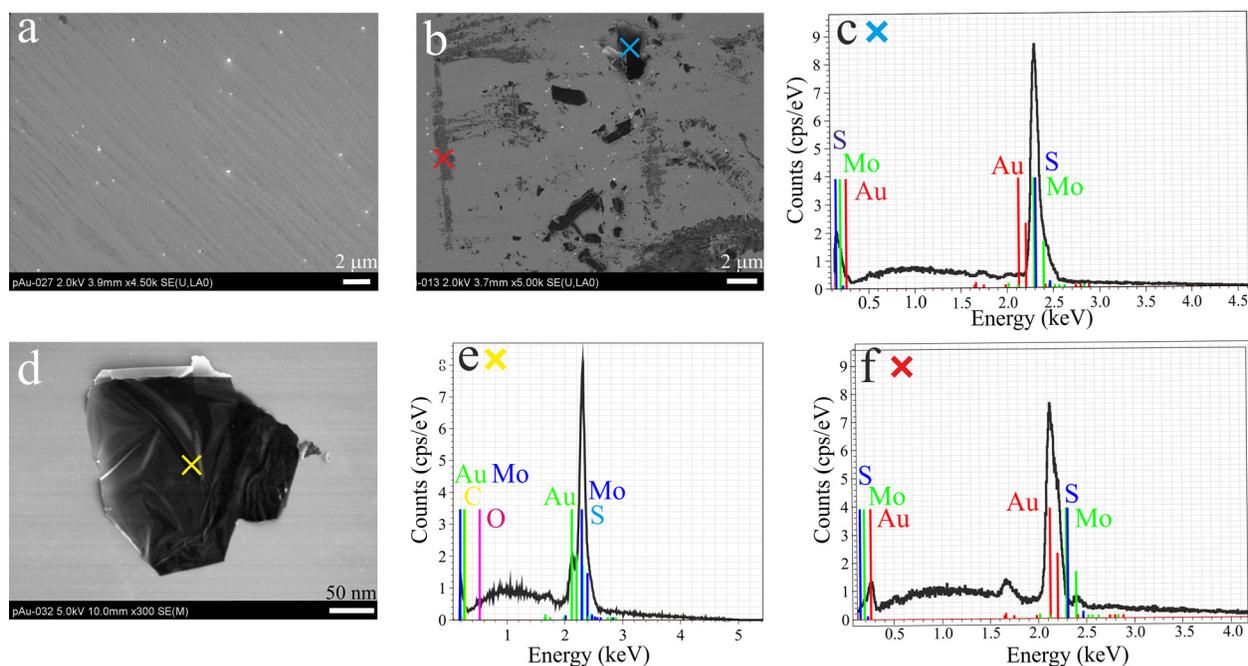
FIG. 6. (Color online) SEM imaging/EDX spectroscopy of the Au(111) target surface after printing. (a) SEM image showing contrast variations due to steps and terraces on the Au surface. (b) Contrast variations indicate the presence of transferred material. (c) and (f) SEM/EDX characterization of the dark features revealed in panel (b) (see crosses). (d) and (e) SEM image and EDX spectrum of a MoS_2 sheet.

induce pillar decapping in a very few spots of the micro-structured area. As a further attempt, the pillar height has been lowered down to about 150 nm, and we also found clear evidences for transferred material from the stamp to target surfaces by combined STM and SEM/EDX measurements. These features are ascribable to crystallites or part of pillars (see supplementary material for details).

The STM characterization of the Au(111) target surface reveals the presence of large and very high clusters, i.e., several hundred of nanometers large in lateral size and 150–200 nm high [as shown in the STM topographies, Figs. 8(a)–8(e)]. It is also very common to find large and structurally rough areas of the Au surface [Figs. 8(f)–8(h)] separated by sharp boundaries from the flat Au areas in the
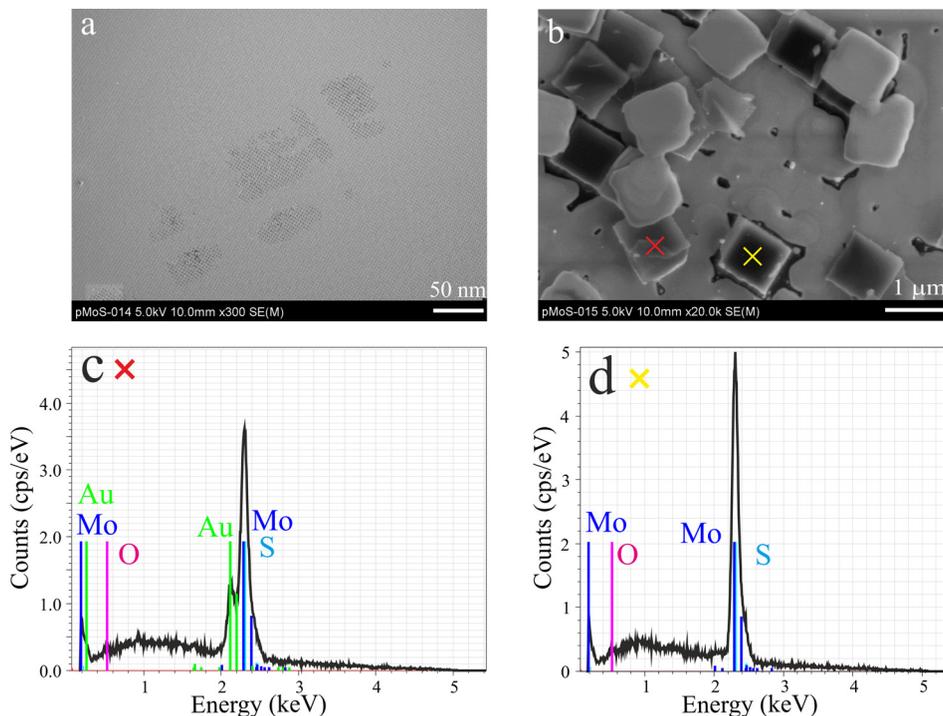

FIG. 7. (Color online) SEM overview and higher resolution image of the stamp surface after printing at large (a) and small scale (b). (c) and (d) EDX spectra taken on top of a decapped pillar (d) and likely a residual of a capping layer (c).
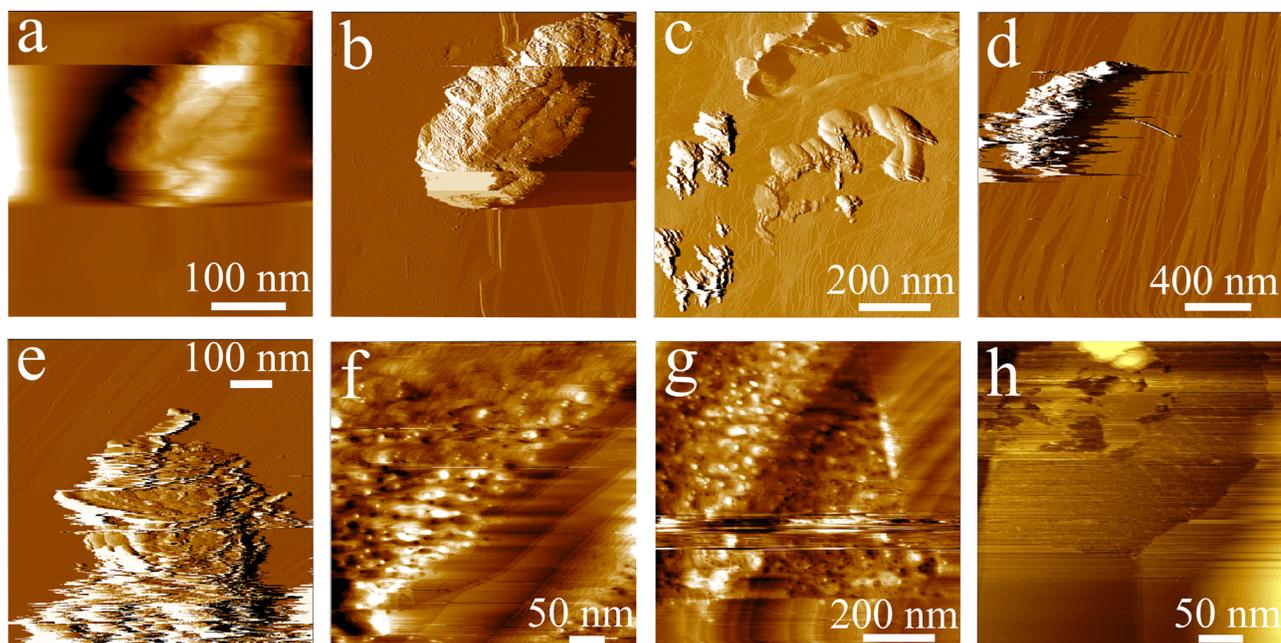
FIG. 8. (Color online) STM characterization of the target Au(111) crystal surface after UHV printing. a) STM image (−2.75 V, 50 pA) and its differential Z height image (b) showing a large and high (about 150 nm) cluster. (c)–(e) Differential Z height STM topographies revealing large and very structured features that might have been transferred while bringing target and stamp surfaces into contact; Set points: (c) and (d): (−2 V, 50 pA), (e): (−2 V, 30 pA). (f)–(h) STM images of large Au(111) surface areas presenting an irregular structure (the border are instead sharply pronounced); Set points: (f) and (g): (−3 V, 30 pA), (h): (−2 V, 30 pA).
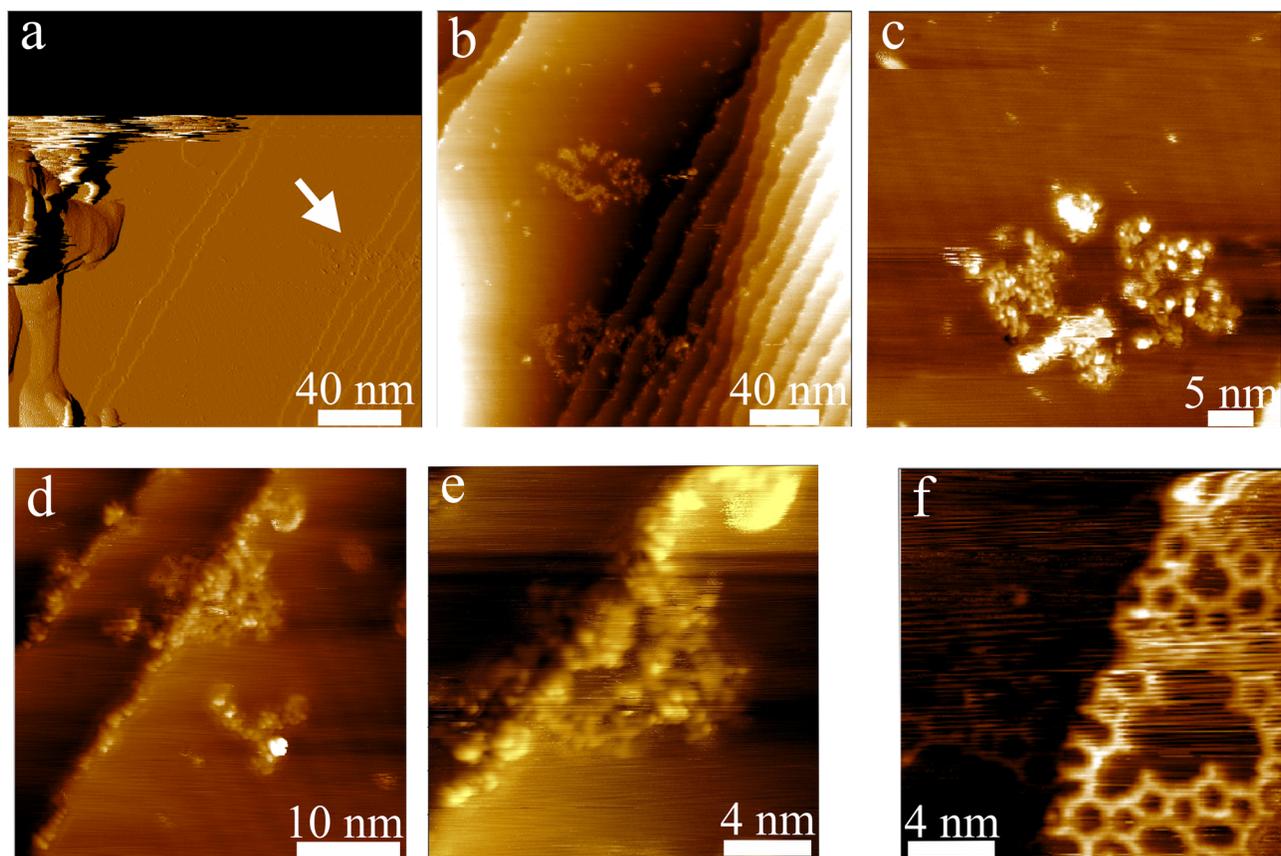
FIG. 9. (Color online) Au(111) target surface after printing. (a)–(e) STM images of small extended carpet-like structures taken on the target surface after printing. These structures are rarely found. Set points: (a) (differential Z height STM image): (−2 V, 10 pA), (b) and (c): (−2 V, 30 pA), (d) and (e): (−1.75 V, 30 pA). (f) TBPB-networks grown on Au(111) [set point: (−2 V, 50 pA)] taken for comparison.

JVST B - Nanotechnology and Microelectronics: Materials, Processing, Measurement, and Phenomena

surrounding [see Figs. 8(f)–8(h)]. Importantly, these features are never found on the clean target surface before printing. They are therefore a result of the contact between the stamp and target surfaces. These large clusters could be Au crystallites that were formed on top of the pillars while growing the thin Au layer and then transferred to the target surface during printing. They also might include part of the pillars themselves, which is hard to distinguish in the STM images. However, it is reasonable to conclude that the mechanical contact between the microstructured stamp and the target surface caused a local material transfer (gold crystallites and potentially pillar fragments) at the pillar positions.

As a consequence of this interpretation, one might find covalent molecular networks just right below them. Displacing those large clusters via STM-based lateral STM manipulation[37,38] turned out to be not possible to achieve—likely due either to the large cluster size or the strong bonding to the surface. Operating the STM tip in lateral (constant-current) manipulation mode caused severe tip modification and no evidence for lateral displacement of the large clusters. Consequently, the search for transferred molecular material in the *vicinity* of these transferred clusters was attempted, and indeed, some carpetlike structures were found in proximity of large clusters in STM images [Fig. 9(a)], albeit rarely. A closer look at the internal structure of these features reveals the lack of a local order and mainly bumpy features, as shown in Figs. 9(b)–9(e). Importantly, such structures were never found on the target surface *before* printing, indicating that they are related to the printing process and therefore probably represent transferred material. Their nonuniform shapes point to organic molecular structures (in contrast to much larger structures with straight edges that are typical for transferred pillar fragments in a crystalline state). Thus, it seems reasonable to assign them to transferred TBPB network patches that slightly changed their appearance during the printing process (either because of additional material from the stamps or because of chemical modification) as visible from a comparison between those identified structures after printing [Figs. 9(c) and 9(e)] and the typical polygonal structure of an intact TBPB network [Fig. 9(f)].

IV. SUMMARY AND CONCLUSIONS

Clear signatures that prove a physical contact between the *stamp* and *target* surfaces have been observed. Indeed, MoS₂ (stamp substrate material) has been transferred to the target surfaces and unambiguously identified by EDX/SEM spectroscopy. Moreover, large clusters have also been found on the target surface by STM and interpreted as Au crystallites or pillar fragments transferred during printing. Molecular nanostructures made of TBPB's or GNR's might reasonably lie under these clusters. Any attempt to laterally displace these clusters by STM-based lateral manipulation turned out to be extremely difficult to achieve likely because of their large size (hundreds of nanometers wide and high). Interesting carpetlike structures were also found in rare cases on the target surface. Importantly, they were never found

before printing and can thus tentatively be assigned to transferred molecular TBPB structures. Their appearance looks different when being compared to intact TBPB networks, which we assign either to the additional transfer of the stamp material or to a chemical modification during printing, hampering a conclusive assessment.

Based on our experiments, the following points should be considered for the efficient transfer of molecular structures under ultraclean conditions: The pillar surfaces should ideally be homogeneous (i.e., without an additional layer on top that might be transferred by mistake), atomically flat, and free of crystallites. The STM technique is fundamental for imaging of the nanostructures before and after printing but requires support from a spectroscopy tool for a chemical characterization of the target and stamp surfaces.

Moreover, the interactions between the polymers and the two samples (stamp and target) during printing are a critical issue. Here, the stamp and target surfaces were both made of gold, thus with similar sticking coefficients for the molecular structures. More or less reactive surfaces can change this balance in favor of one of the two samples, due to the different adsorption energies. While the lamellar structure of MoS₂ provides the softness required to absorb the applied force while pressing the stamp against the target, the weakly interacting MoS₂ layers can also be easily displaced from each other, resulting in fragmentation or decapping as seen in our experiments. More stable, yet still soft, stamp materials are therefore advantageous.

A further issue to be improved for an efficient transfer is the surface of the pillars that should ideally be atomically flat, which is not the case in the current study, due to the formation of Au crystallites. This can reduce the diffusion of molecular species on the pillar surface, a key-ingredient for the successful *in situ* synthesis of molecular species. Furthermore, Au crystallites can be transferred to the target surfaces—as seen in our experiments—and represent undesired extra-material there, hampering the search for transferred molecular structures.

ACKNOWLEDGMENT

[1]J. R. Heath and M. A. Ratner, Phys. Today **56**, 43 (2003).
[2]T. Zambelli, J. V. Barth, and J. Wintterlin, J. Phys.: Condens. Matter **14**, 4241 (2002).
[3]L. Grill, K.-H. Rieder, F. Moresco, G. Rapenne, S. Stojkovic, X. Bouju, and C. Joachim, Nat. Nanotechnol. **2**, 95 (2007).
[4]S. Höger, Chem. Eur. J. **10**, 1320 (2004).
[5]L. Zhi and K. Müllen, J. Mater. Chem. **18**, 1472 (2008).
[6]L. Lafferentz, V. Eberhardt, C. Dri, C. Africh, G. Comelli, F. Esch, S. Hecht, and L. Grill, Nat. Chem. **4**, 215 (2012).
[7]J. A. Lipton-Duffin, O. Ivasenko, D. F. Perepichka, and F. Rosei, Small **5**, 592 (2009).
[8]J. Cai *et al.*, Nature **466**, 470 (2010).
[9]M. Koch, F. Ample, C. Joachim, and L. Grill, Nat. Nanotechnol. **7**, 713 (2012).
[10]J. F. Dienstmaier, A. M. Gigler, A. J. Goetz, P. Knochel, T. Bein, A. Lyapin, S. Reichlmaier, W. M. Heckl, and M. Lackinger, ACS Nano **5**, 9737 (2011).

[11]A. Gourdon, Angew. Chem.-Int. Ed. **47**, 6950 (2008).

[12]M. Lackinger and W. M. Heckl, J. Phys. D: Appl. Phys. **44**, 464011 (2011).

[13]J. Méndez, M. F. López, and J. A. Martín-Gago, Chem. Soc. Rev. **40**, 4578 (2011).

[14]M. El Garah, J. M. MacLeod, and F. Rosei, Surf. Sci. **613**, 6 (2013).

[15]R. Gutzler, H. Walch, G. Eder, S. Kloft, W. M. Heckl, and M. Lackinger, Chem. Comm. 4456 (2009).

[16]J. A. Lipton-Duffin, J. A. Miwa, M. Kondratenko, F. Cicoira, B. G. Sumpter, V. Meunier, D. F. Perepichka, and F. Rosei, PNAS **107**, 11200 (2010).

[17]M. Bieri *et al.*, J. Am. Chem. Soc. **132**, 16669 (2010).

[18]M. Kolmer, A. A. A. Zebari, J. S. Prauzner-Bechcicki, W. Piskorz, F. Zasada, S. Godlewski, B. Such, Z. Sojka, and M. Szymonski, Angew. Chem. Int. Ed. **52**, 10300 (2013).

[19]M. Kolmer *et al.*, Chem. Commun. **51**, 11276 (2015).

[20]R. Lin, M. Galili, U. J. Quaade, M. Brandbyge, T. Bjornholm, A. D. Esposti, F. Biscarini, and K. Stokbro, J. Chem. Phys. **117**, 321 (2002).

[21]N. A. Melosh, A. Boukai, F. Diana, B. Gerardot, A. Badolato, P. M. Petroff, and J. R. Heath, Science **300**, 112 (2003).

[22]A. J. Pollard *et al.*, J. Phys. Chem. C **113**, 16565 (2009).

[23]M. B. Wieland, A. G. Slater, B. Mangham, N. R. Champness, and P. H. Beton, Beilstein J. Nanotechnol. **5**, 394 (2014).

[24]A. K. Geim and I. V. Grigorieva, Nature **499**, 419 (2013).

[25]J. Kang, D. Shin, S. Bae, and B. H. Hong, Nanoscale **4**, 5527 (2012).

[26]J. Deng, C. Troadec, and C. Joachim, IOP Conf. Ser.: Mater. Sci. Eng. **6**, 012033 (2009).

[27]J. Deng, C. Troadec, H. K. Hui, and C. Joachim, J. Vac. Sci. Technol. B **28**, 484 (2010).

[28]R. J. Hamers, R. M. Tromp, and J. E. Demuth, Phys. Rev. Lett. **56**, 1972 (1986).

[29]R. M. Feenstra, J. A. Stroscio, and A. P. Fein, Surf. Sci. **181**, 295 (1987).

[30]See supplementary material at http://dx.doi.org/10.1116/1.4936886 for information about the preparation and the surface roughness characterization of the MoS$_2$ substrate surface as well as the characterization of 2D-TBPB networks on and off the top pillar surfaces. We included also a combined STM-SEM/EDX study of the printing transfer of graphene nanoribbons from a microstructured stamp surface to a single crystal target Au(111) surface.

[31]S. Weigelt *et al.*, Angew. Chem.-Int. Ed. **46**, 9227 (2007).

[32]S. A. Krasnikov, C. M. Doyle, N. N. Sergeeva, A. B. Preobrajenski, N. A. Vinogradov, Y. N. Sergeeva, A. A. Zakharov, M. O. Senge, and A. A. Cafolla, Nano Res. **4**, 376 (2011).

[33]M. O. Blunt, J. C. Russel, N. R. Champness, and P. H. Beton, Chem. Commun. **46**, 3 (2010).

[34]G. Eder, E. F. Smith, I. Cebula, W. M. Heckl, P. H. Beton, and M. Lackinger, ACS Nano **7**, 3014 (2013).

[35]Z.-J. Wang *et al.*, ACS Nano **9**, 1506 (2015).

[36]G. P. Lopez, H. A. Biebuyck, and G. M. Whitesides, Langmuir **9**, 1513 (1993).

[37]G. Meyer, L. Bartels, S. Zöphel, E. Henze, and K. H. Rieder, Phys. Rev. Lett. **78**, 1512 (1997).

[38]C. Bombis, F. Ample, J. Mielke, M. Mannsberger, C. J. Villagómez, C. Roth, C. Joachim, and L. Grill, Phys. Rev. Lett. **104**, 185502 (2010).